The use of the Sudden Ionospheric Disturbance Radio Telescope to predict the signal and observe the North American 2017 Total Solar Eclipse

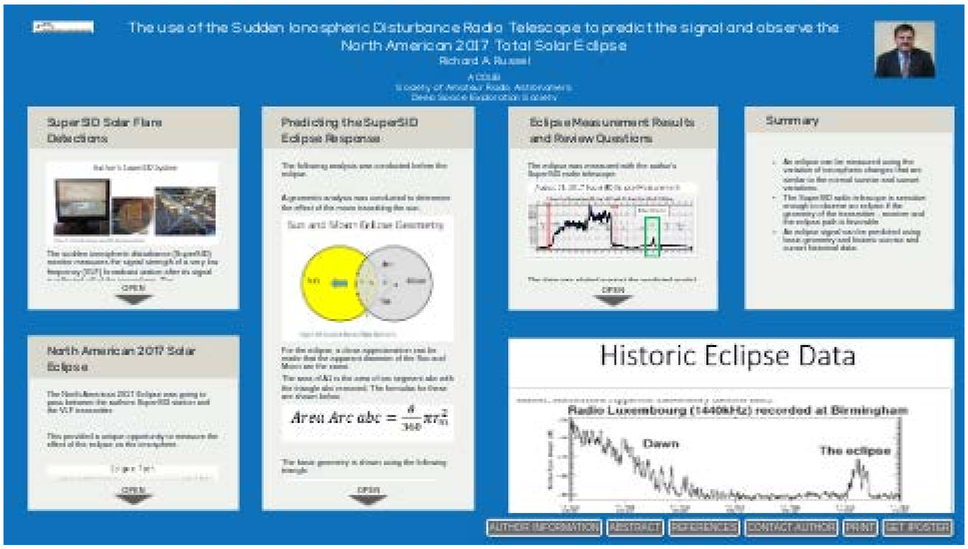

Richard A. Russel

AC0UB
Society of Amateur Radio Astronomers
Deep Space Exploration Society

PRESENTED AT:

SUPERSID SOLAR FLARE DETECTIONS

Author’s SuperSID System

Figure 2: Colorado Springs SuperSID Monitoring Station

The sudden ionospheric disturbance (SuperSID) monitor measures the signal strength of a very low frequency (VLF) broadcast station after its signal is reflected off of the ionosphere. The characteristics of the signal strength is highly dependent on the local night and day. The Sun’s energy ionizes the Earth’s atmosphere during the day. This produces different ionization layers defined as layers D, E, F. At night, there is only ionization from cosmic waves, and therefore there is only an F layer (1).

VLF radio waves reflect off the free electrons in the different ionosphere layers. The signal strength of this reflected signal can be detected by a SuperSID small radio telescope. The normal use of the SuperSID radio telescope is to detect solar flares which appear as short term signal strength increases during the daytime monitoring.

The author used the SuperSID telescope’s capability to measure and analyze the VLF signal strength variations and the effect of the solar eclipse on the ionosphere. The total solar eclipse on August 21, 2017 in North America provides an opportunity to analyze the differences between the eclipse and normal daily ionospheric reflections.

Example solar flares detected by the author's SuperSID radio telescope.

Detections of M and X Flares

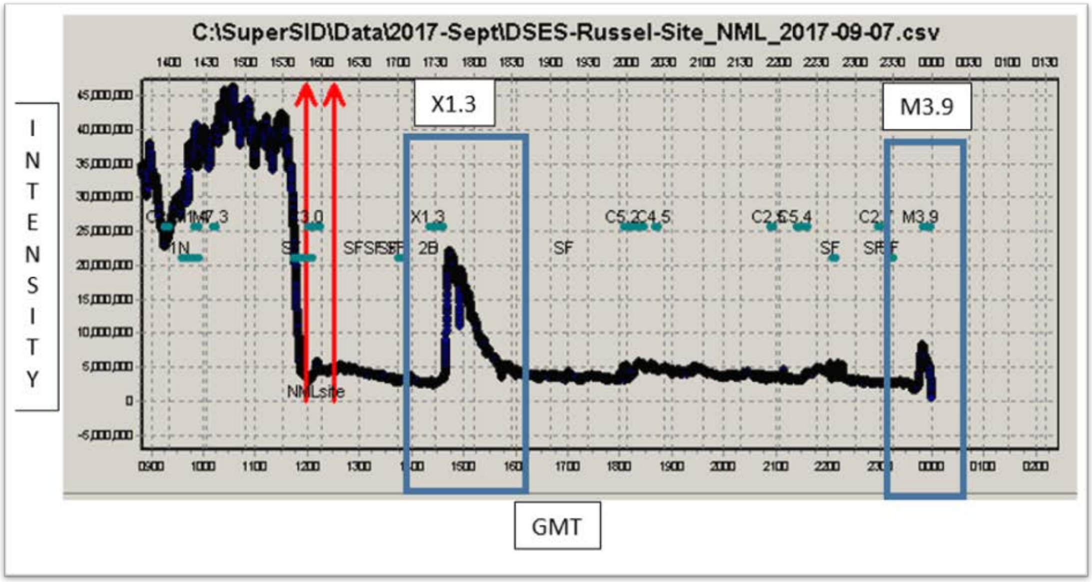
C:\SuperSID\Data\2017-Sept\DSES-Russel-Site_NML_2017-09-07.csv
X1.3
M3.9
INTENSITY
GMT

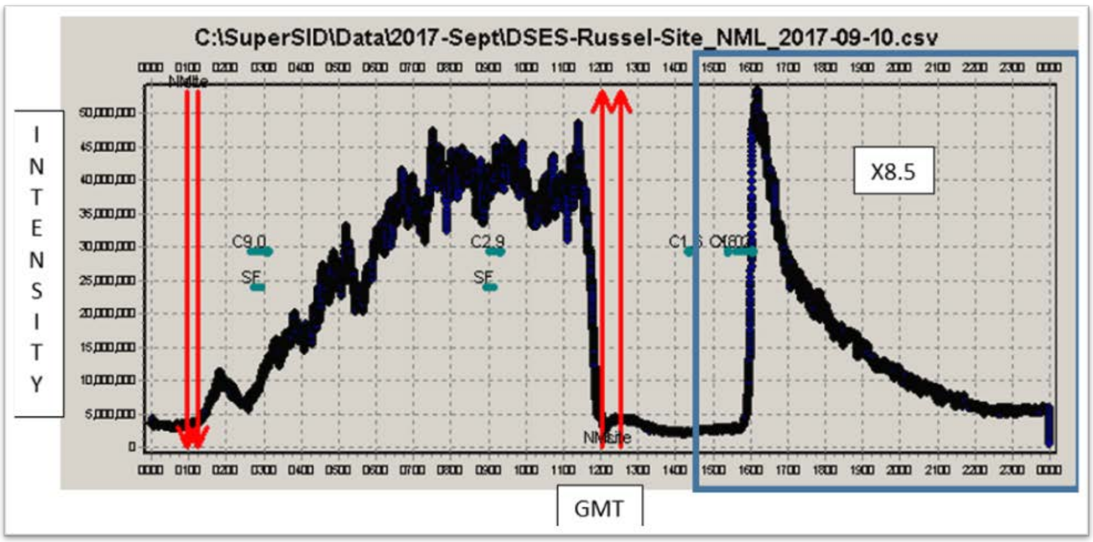
C:\SuperSID\Data\2017-Sept\DSES-Russel-Site_NML_2017-09-10.csv
X8.5
INTENSITY
GMT

NORTH AMERICAN 2017 SOLAR ECLIPSE

The North American 2017 Eclipse was going to pass between the authors SuperSID station and the VLF transmitter.

This provided a unique opportunity to measure the effect of the eclipse on the ionosphere.

Figure 18: Eclipse Path (7) (8)

PREDICTING THE SUPERSID ECLIPSE RESPONSE

The following analysis was conducted before the eclipse.

A geometric analysis was conducted to determine the effect of the moon transitting the sun.

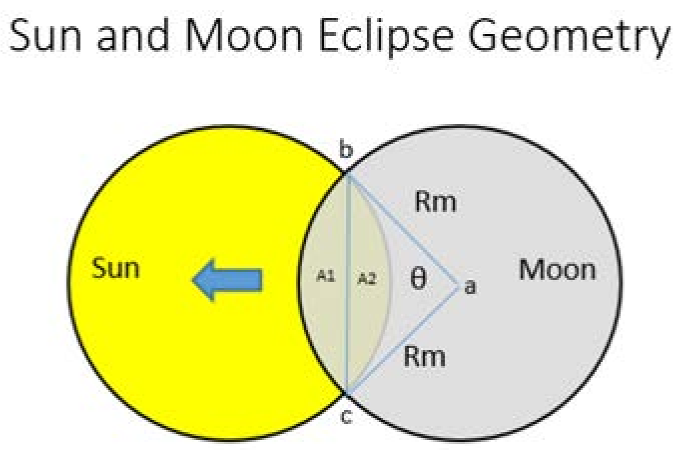

Figure 20: Sun and Moon Eclipse Geometry

For the eclipse, a close approximation can be made that the apparent diameter of the Sun and Moon are the same.

The area of A1 is the area of arc segment abc with the triangle abc removed. The formulas for these are shown below.

$$Area\ Arc\ abc = \frac{\theta}{360}\pi r_m^2$$

The basic geometry is shown using the following triangle.

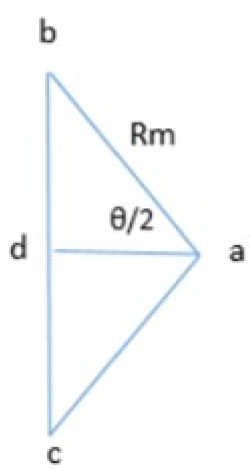

The detailed calcultions are as follows:

Area Δabc = (2) Area Δabd (3)

Note that Δabc is an isosceles triangle with lines ab and ac being equal with central angle θ. By finding the line ad and line bd, the area of Δabd can be found. Note that Rm is the Apparent Moon radius.

Line ad = (Rm) cos(θ/2) (4)

Line bd = (Rm) sin((θ/2) (5)

The area of Δabc is therefore:

$$\text{Area } \Delta abc = (2)\text{Area } \Delta abd = (2)\frac{1}{2}(R_m^2)\cos\left(\frac{\theta}{2}\right)\sin\left(\frac{\theta}{2}\right) = (R_m^2)\cos\left(\frac{\theta}{2}\right)\sin\left(\frac{\theta}{2}\right) \quad (6)$$

Finally, the area of A1 is:

Area A1 = Area arc abc - Area Δabc (7)

Assume that the apparent radius of the Moon is the same as the apparent radius of the Sun for the eclipse. Therefore, the area A1 = A2. So, the total eclipse area can now be calculated as:

$$Total\ Eclipse\ Area = (2)Area\ A1 = (2)\left(\frac{\theta}{360}\pi r_m^2 - (\boldsymbol{R_m^2})\boldsymbol{cos}\left(\frac{\theta}{2}\right)\boldsymbol{sin}\left(\frac{\theta}{2}\right)\right) \quad (8)$$

$$Total\ Eclipse\ Area = r_m^2\left(\frac{\theta}{180}\pi - 2\boldsymbol{cos}\left(\frac{\theta}{2}\right)\boldsymbol{sin}\left(\frac{\theta}{2}\right)\right) \quad (9)$$

The data was calibrated based on the NASA time prediction of the eclipse transit.

Calculations for Sun Eclipse Time

Time	Delta Time (Min)	Theta (deg)	% Sun Eclipsed
16:30	0	0.0	0.0%
16:38	8	18.0	0.2%
16:47	17	36.0	1.3%
16:55	25	54.0	4.2%
17:03	33	72.0	9.7%
17:12	42	90.0	18.2%
17:20	50	108.0	29.7%
17:28	58	126.0	44.2%
17:37	67	144.0	61.3%
17:45	75	162.0	80.2%
17:54	84	180.0	100.0%
18:02	92	162.0	80.2%
18:10	100	144.0	61.3%
18:19	109	126.0	44.2%
18:27	117	108.0	29.7%
18:35	125	90.0	18.2%
18:44	134	72.0	9.7%
18:52	142	54.0	4.2%
19:00	150	36.0	1.3%
19:09	159	18.0	0.2%
19:17	167	0.0	0.0%

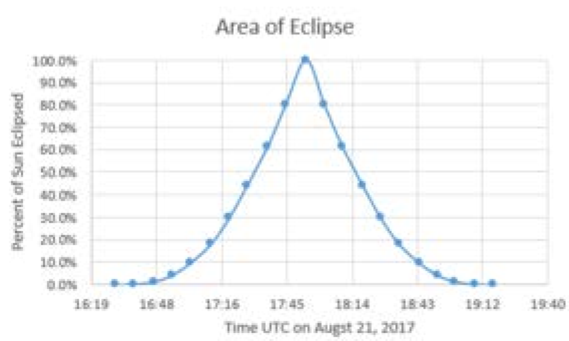

The next step was to model the SuperSID response to sunrise and sunset. This analysis would correlate to the eclipse percentages.

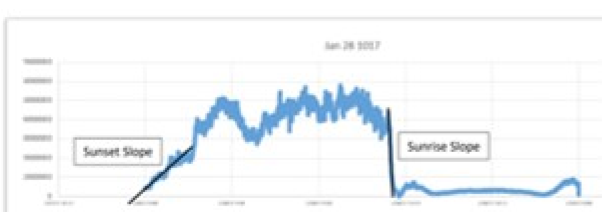

Figure 4: SID Monitor Output for January 28, 2017

Averaging multiple sunrise and sunset measurements resulted in the following historical measurement model calibrated to the eclipse transit time.

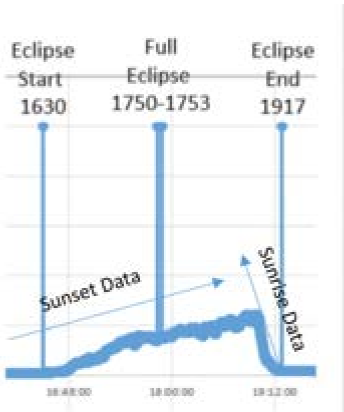

The last prediction step was to combine the models and add an historical SuperSID measurement that closely represented the normal day and night response.

Th results of the historic data was calibrated to the eclipse time.

Time	Delta Time (Min)	Theta (deg)	% Sun Eclipsed	Rate Analysis (Units)
16:30	0	0.0	0.0%	799,905
16:38	8	18.0	0.2%	805,178
16:47	17	36.0	1.3%	851,939
16:55	25	54.0	4.2%	988,797
17:03	33	72.0	9.7%	1,302,155
17:12	42	90.0	18.2%	1,960,647
17:20	50	108.0	29.7%	2,918,317
17:28	58	126.0	44.2%	4,343,799
17:37	67	144.0	61.3%	6,565,112
17:45	75	162.0	80.2%	9,147,633
17:54	84	180.0	100.0%	12,771,887
18:02	92	162.0	80.2%	12,397,322
18:10	100	144.0	61.3%	8,601,185
18:19	109	126.0	44.2%	854,789
18:27	117	108.0	29.7%	(8,663,455)
18:35	125	90.0	18.2%	(20,277,034)
18:44	134	72.0	9.7%	(33,421,077)
18:52	142	54.0	4.2%	(47,558,362)
19:00	150	36.0	1.3%	(62,231,897)
19:09	159	18.0	0.2%	(77,109,662)
19:17	167	0.0	0.0%	(92,017,100)

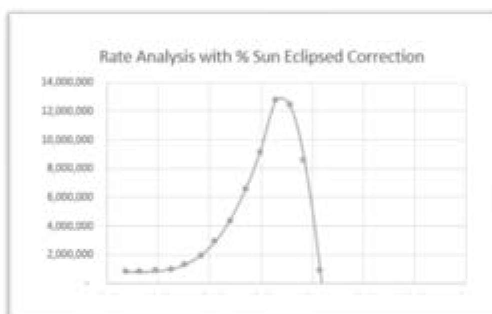

Figure 24: Rate Data Corrected with Sun Area (Corrected)

The combined prediction model is shown below

Combined Model Detail

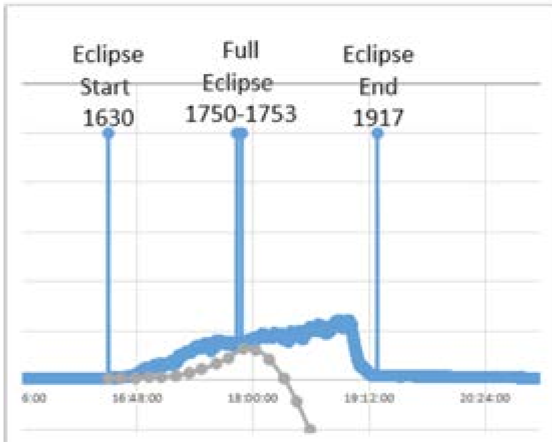

ECLIPSE MEASUREMENT RESULTS AND REVIEW QUESTIONS

The eclipse was measured with the author's SuperSID radio telescope.

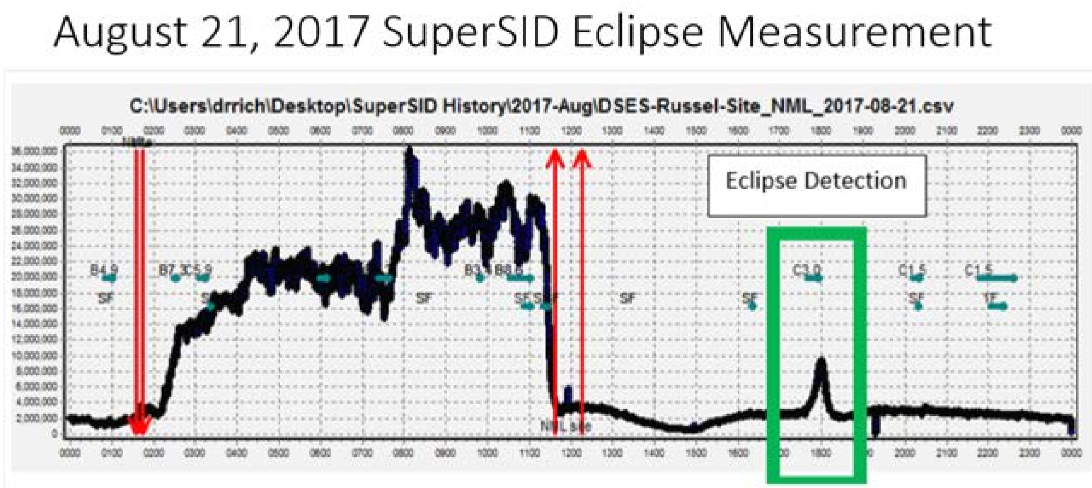

The data was plotted against the predicted model with excellent correlation.

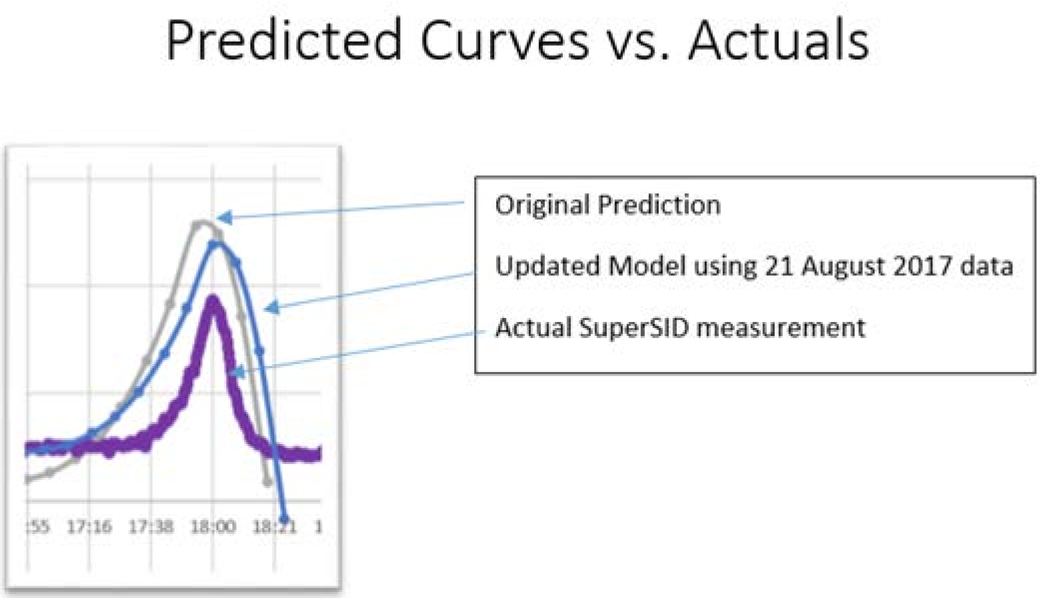

Detailed Questions

#1 Could you add some more detail explaining the physics of why we see the amplitude increase at night?

- **Normal VLF Propagation**

When a radio wave is transmitted, the radio wave propagates through either the:

- Ground wave or
- Sky wave.

The **ground wave** travels near the earth's surface and is quickly absorbed.

The **sky wave** travels through the ionosphere bouncing back and forth for as much as 2 or 3 times. The SID monitors pick up the sky waves which have traveled through the ionosphere.

The highly stratified layers of the ionosphere refract the VLF waves until the angle of incidence of the wave reaches the critical frequency. After the critical frequency, the wave gets reflected back to earth.

During the Day:
The ionization density of about 1000 electrons/cm^3 of the D-layer is not enough to reflect the VLF waves. During the day, the waves pass through the D-layer are reflected by the highly ionized E and F layers. While, the density of the D-layer is not enough to reflect the VLF waves, the D-layer is partially ionized and this partially ionized D-layer attenuates the signal to some extent

During the Night:
In the absence of the solar radiation, the D-layer disappears during the night. Now, the VLF waves travel to the E and F layers where it gets reflected back. There is no lightly ionized D-layer to attenuate the signal and the signal strength is higher than that during the day. Graph 3 illustrates this difference.

Source: [Space Weather Monitors- Stanford SOLAR Center] Sharad Khanal

71

Detailed Questions

#2 I know there is a C3 class flare that happened right during the eclipse. Could you add some discussion as to how it does or does not affect your results?

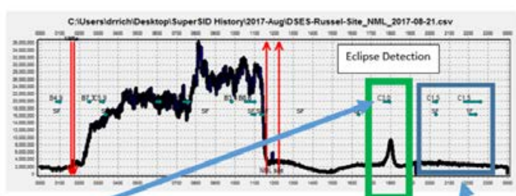

Figure 8: August 21, 2017 Eclipse data

Note the C3.0 flare that was detected by the GOES Satellites that corresponded to the eclipse time. The SuperSID is barely sensitive to low C class flares as can be seen by the two C1.5 flares to the right of the eclipse. Therefore, the C3.0 flare was not considered as a significant contributor to the eclipse signal.

72

Detailed Questions

#3 Can you add ticks and axes labels to your model detail and predicted vs actual figures?

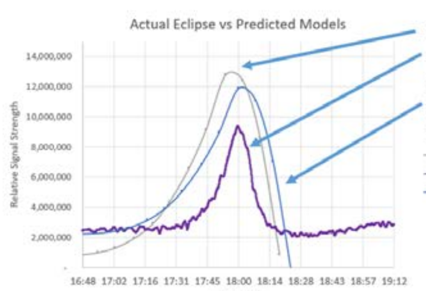

Calculated: Original predictive model May 2017 prediction
Aug 21 – Eclipse: Actual eclipse measurement on Aug 21, 2017
Aug 21 new predict: Updated prediction model based on better actual eclipse time

73

Detailed Questions

#4 What are some reasons that account for the differences in observations vs model?

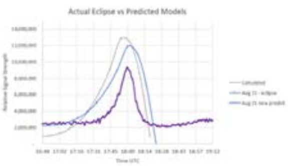

- The actual eclipse signal did not have as high of gain as the model predicted.
  - The model used historic sunset and sunrise rates. The eclipse sunset rate appears to be lower than the historic average. This is possibly because the entire sky is not going dark, just the area of the eclipse.
- The peak time was off in the original model from the actual eclipse
  - The original model peak time was an estimate of when the eclipse would pass between the transmitter and SuperSIDS sight. This was roughly calculated on a map using NASA time predictions. The updated prediction just moved the peak to the actual peak eclipse time

SUMMARY

- An eclipse can be measured using the variation of ionospheric changes that are similar to the normal sunrise and sunset variations.
- The SuperSID radio telescope is sensitive enough to observe an eclipse if the geometry of the transmitter - receiver and the eclipse path is favorable
- An eclipse signal can be predicted using basic geometry and historic sunrise and sunset historical data.

Ionospheric Variation During Sunrise and Sunset and Predictions and Results for the 2017 Total Eclipse

Purpose

- The presentation is based on two separate presentations:
  - One before the eclipse which developed the eclipse prediction model for the SuperSID radio telescope
  - The second showed the successful eclipse measurements and the close correlation with the measurement and the predictive model
- Goals
  - Predict the SuperSID output during the 2017 Solar Eclipse
  - Use SuperSID historic data from 1 year of data
    - Uses NASA predicted start and stop times plus historic SuperSID data to predict output during eclipse
  - Calculate the sunrise and sunset historic rise and fall rates
    - Develop eclipse shadowing geometry
    - Apply rates to shadowing to develop the prediction model
  - Show the results of the measurements and compare with the predictive model

Historic Eclipse Data

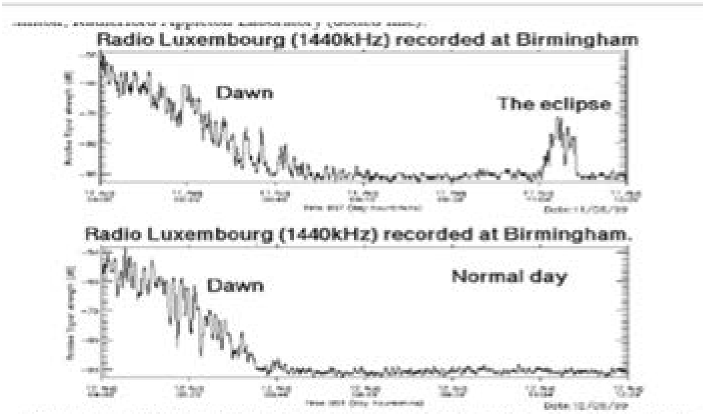

Figure 19. A plot of the variation in the received CW radio signal as recorded in Birmingham RA Regional Office in the UK of the 1440kHz (±1.4kHz) carrier emanating from Radio Luxembourg at Marnach (a) for the morning of the total eclipse and (b) the day after the eclipse.

Author's SuperSID System

Figure 2: Colorado Springs SuperSID Monitoring Station

Appendix A - VLF Station List[10]

See http://sidstation.lionelloudet.homedns.org/stations-list-en.xhtml for a current version of this list.

Country	Location	Name	Frequency	Power (kHz)	Latititude / Longitude
USA	Cutler, ME	NAA	24.0	1000	44.65 N -67.3 W
	Jim Creek, WA	NLK	24.8	250	48.20 N -121.92 W
	Lualualei, HI	NPM	21.4	566	20.4 N -158.2 W
	LaMoure, ND	NML	25.2	500	46.35 N -98.33 W
	Aquada, Puerto Rico	NAU	40.75	100	18.40 N -67.18 W
Antarctica:	South Pole	VLF	20.0		-09 / 0
Australia	Harold E. Holt (North West Cape)	NWC	19.8	1000	-21.8 114.2 E
China[11]:	Changde	3SA (alternates 3SB)	20.6		25.03 111.67
	Datonge	3SB (alternates 3SA)	10.6		35.60 103.33
France:	Rosnay	HWU	20.9	400	40.7N 1.25E
	St. Assie	FTA[12]	16.8		
	LeBlanc (NATO)	HWV	21.75		40.7 N, 1.25 E
Germany:	Rhauderfehn	DHO	23.4	500	53° 10' N 07° 33'E
Iceland:	Keflavik (US Navy)	NRK	37.5	100	65N -18E
	Keflavic	TFK	37.5		
India:	Katabomman	VTX3	18.2		8.47 77.40
Italy:	Tavolara	ICV	20.27	43	40.88N 9.68E
	Sicily	NSC	45.9		38N 13.5E
Japan:	Ebino	JJI	22.2		32.04 130.81
Norway[13]:	Kolsas	JXN	16.4	45	59.51N 10.52E
Russia[14]:	Arkhanghelsk	UGE	19.7	150 input	64N24 41E32
	Batumi	UVA	14.6	100 input	
	Kaliningrad	UGKZ	30.3	100 input	
	Matotchkinchar	UFQE	18.1	100 input	
	Vladivostok	UIK	15.0	100 input	
Turkey	Bafa	TBB	26.7		37.43 27.55
United Kingdom	Anthorn	GBZ	19.6	500	52:71N -3:07W
	Anthorn (NATO)	GQD	22.1	500	52:4N -1.2W
	London	GYA	21.37	120	51 N 2 E

There is no transmitter below 18.3 kHz usable for SID monitoring in Europe.

LaMoore, ND

Figure 3: VLF Station List (1)

Typical SuperSID 24-hour Day

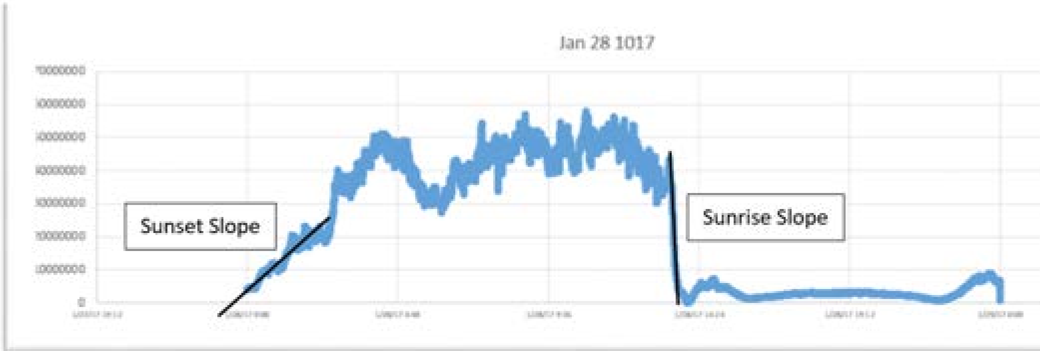

Figure 4: SID Monitor Output for January 28, 2017

Data Collection Sunrise and Sunset

Parameter	Value		Date	Transmitter Sunrise	Receiver Sunrise	Start Time	Stop Time	Delta Time	Start Level	Stop Level	Delta Level	Rate per second
Sunrise Rate Mean	(15,742)		1-Jan-17		14:09	13:30	14:09	1950	15,744,646	1,352,493	(18,292,153)	(9,888)
Sunrise Rate Stdev	5,493	-34.9%	2-Jan-17			13:30	13:50	1200	14,838,240	1,786,396	(13,051,842)	(10,877)
Sunset Rate Mean			3-Jan-17			13:46	14:10	1440	13,057,672	64,961	(12,992,689)	(9,023)
Sunset Rate StDev			4-Jan-17			13:38	14:03	1500	24,122,296	108,527	(24,013,478)	(16,009)
			5-Jan-17			13:43	14:04	1260	17,580,796	498,343	(17,082,448)	(13,557)
			6-Jan-17			13:38	14:04	1320	30,604,060	660,059	(29,944,005)	(22,685)
			7-Jan-17			13:29	14:04	1500	32,045,405	1,599,783	(30,445,622)	(20,297)
			8-Jan-17			13:31	14:02	1800	37,901,601	1,194,586	(36,107,298)	(20,104)
			9-Jan-17			13:28	14:00	1920	29,712,508	2,317,404	(27,395,104)	(19,477)
			10-Jan-17			13:15	14:06	3060	40,254,206	721,819	(39,532,387)	(12,919)

Figure 5: Sunrise Rate Analysis Data – January 2017

Parameter	Value		Date	RCV Sunrise UTC	Receiver Sunset Time	Start Time	Stop Time	Delta Time	Start Level	Stop Level	Delta Level	Rate per second
Sunset Rate Mean	3,706		1-Jan-17									
Sunset Rate Stdev	831	22.4%	2-Jan-17	[illegible]	23:26	23:26	0:26	3360	[illegible]	[illegible]	[illegible]	[illegible]
			3-Jan-17	[illegible]	[illegible]	[illegible]	[illegible]	[illegible]	[illegible]	[illegible]	[illegible]	[illegible]
			4-Jan-17	[illegible]	[illegible]	[illegible]	[illegible]	[illegible]	[illegible]	[illegible]	[illegible]	[illegible]
			5-Jan-17	[illegible]	[illegible]	[illegible]	[illegible]	[illegible]	[illegible]	[illegible]	[illegible]	[illegible]
			6-Jan-17	[illegible]	[illegible]	[illegible]	[illegible]	[illegible]	[illegible]	[illegible]	[illegible]	[illegible]
			7-Jan-17	[illegible]	[illegible]	[illegible]	[illegible]	[illegible]	[illegible]	[illegible]	[illegible]	[illegible]
			8-Jan-17	[illegible]	23:40	23:40	[illegible]	3000	[illegible]	[illegible]	[illegible]	[illegible]
			9-Jan-17	[illegible]	[illegible]	[illegible]	[illegible]	[illegible]	[illegible]	[illegible]	[illegible]	[illegible]
			10-Jan-17	[illegible]	[illegible]	[illegible]	[illegible]	[illegible]	[illegible]	[illegible]	[illegible]	[illegible]

Figure 6: Sunset Rate Analysis - January 2017

Sunrise Control Chart

Date Range	Mean	UCL	LCL
1/1/2017	(15,742)	(10,249)	(21,235)
1/31/2017	(15,742)	(10,249)	(21,235)

Figure 7: January 2017 Sunrise Control Chart

Sunset Control Chart

Date Range	Mean	UCL	LCL
1/1/2017	3,705	4,536	2,873
1/31/2017	3,705	4,536	2,873

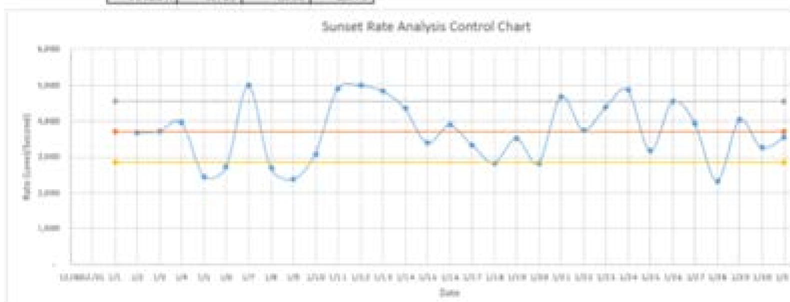

Figure 8: January 2017 Sunset Control Chart

Sunset and Sunrise Rate Averages

SUNSET			SUNRISE	
Date	Units/Second		Date	Units/Second
8/1/2016	11,972		8/1/2016	(35,489)
9/2/2016	14,304		9/2/2016	(71,812)
10/1/2016	9,472		10/1/2016	(79,216)
11/1/2016	6,752		11/1/2016	(20,391)
12/1/2016	3,701		12/1/2016	(21,334)
1/1/2017	4,726		1/1/2017	(11,529)
2/1/2017	4,449		2/1/2017	(11,408)
3/1/2017	4,243		3/1/2017	(32,054)
4/1/2017	2,327		4/1/2017	(9,612)
5/1/2017	5,170		5/1/2017	(17,727)
Average	6,712		Average	(31,057)
STDEV	3,927		STDEV	24,976

Figure 9: Monthly Rates for Sunrise and Sunset

Eclipse Basics

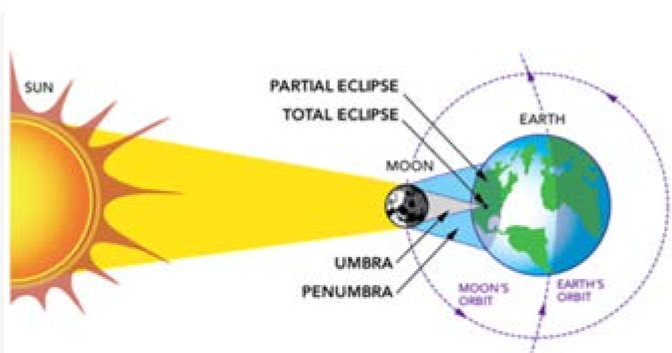

Figure 17:Eclipse Basics (6)

Eclipse Path

Figure 18: Eclipse Path (7) (8)

Eclipse Schedule

	Eclipse Begins	Totality Begins	Totality Ends	Eclipse Ends	
Madras, OR	09:06 a.m.	10:19 a.m.	10:21 a.m.	11:41 a.m.	PDT
Idaho Falls, ID	10:15 a.m.	11:33 a.m.	11:34 a.m.	12:58 p.m.	MDT
Casper, WY	10:22 a.m.	11:42 a.m.	11:45 a.m.	01:09 p.m.	MDT
Lincoln, NE	11:37 a.m.	01:02 p.m.	01:04 p.m.	02:29 p.m.	CDT

Figure 19: Eclipse Schedule (9)

Sun and Moon Eclipse Geometry

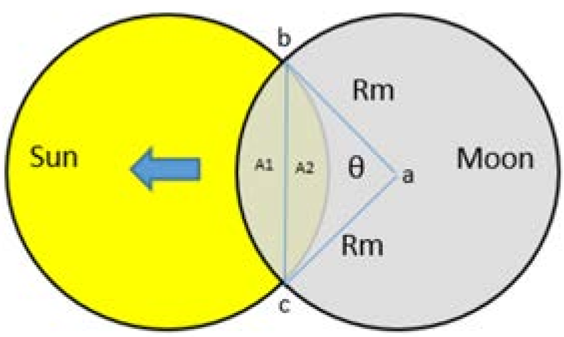

Figure 20: Sun and Moon Eclipse Geometry

Percent Sun Eclipsed

$$Total\ Eclipse\ Area = (2)Area\ A1 = (2)\left(\frac{\theta}{360}\pi r_m^2 - (R_m^2)\cos\left(\frac{\theta}{2}\right)\sin\left(\frac{\theta}{2}\right)\right) \quad (8)$$

$$Total\ Eclipse\ Area = r_m^2\left(\frac{\theta}{180}\pi - 2\cos\left(\frac{\theta}{2}\right)\sin\left(\frac{\theta}{2}\right)\right) \quad (9)$$

The analysis requires the calculation of the percent of the Sun that is eclipsed over time. Using the assumption that for the eclipse Rm = Rs (Sun's apparent radius):

$$Percent\ Sun\ Eclipsed = \frac{Total\ Eclipse\ Area}{Total\ Sun\ Area} = \frac{r_m^2\left(\frac{\theta}{180}\pi - 2\cos\left(\frac{\theta}{2}\right)\sin\left(\frac{\theta}{2}\right)\right)}{\pi r_s^2} \quad (10)$$

With Rm = Rs

$$Percent\ Sun\ Eclipsed = \frac{\theta}{180} - \frac{2}{\pi}\cos\left(\frac{\theta}{2}\right)\sin\left(\frac{\theta}{2}\right) \quad (11)$$

Equation 11 allows for the calculation of the percentage of the Sun that is being eclipsed without knowing the apparent radius of either the Sun or the Moon.

Time	Delta Time (Min)	Theta (deg)	% Sun Eclipsed
16:30	0	0.0	0.0%
16:38	8	18.0	0.2%
16:47	17	36.0	1.3%
16:55	25	54.0	4.2%
17:03	33	72.0	9.7%
17:12	42	90.0	18.2%
17:20	50	108.0	29.7%
17:28	58	126.0	44.2%
17:37	67	144.0	61.3%
17:45	75	162.0	80.2%
17:54	84	180.0	100.0%
18:02	92	162.0	80.2%
18:10	100	144.0	61.3%
18:19	109	126.0	44.2%
18:27	117	108.0	29.7%
18:35	125	90.0	18.2%
18:44	134	72.0	9.7%
18:52	142	54.0	4.2%
19:00	150	36.0	1.3%
19:09	159	18.0	0.2%
19:17	167	0.0	0.0%

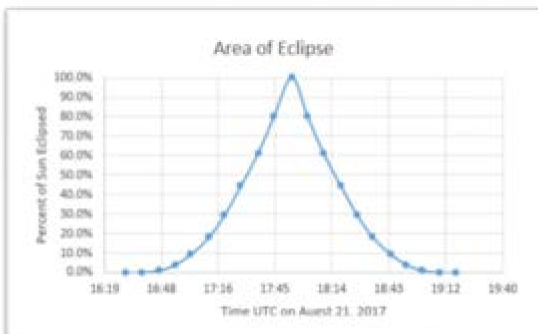

Prediction using Historic Data

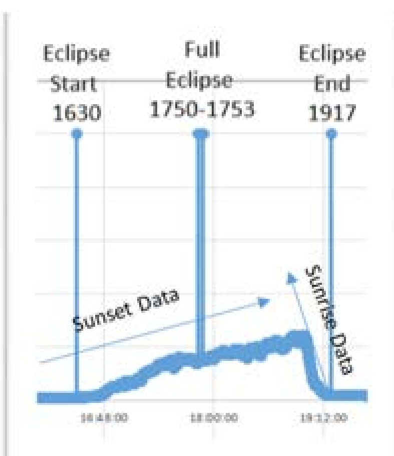

Figure 23: Historic Model

Predicted Model using Calculations and Rate Data

Time	Delta Time (Min)	Theta (deg)	% Sun Eclipsed	Rate Analysis (Units)
16:30	0	0.0	0.0%	799,905
16:38	8	18.0	0.2%	805,178
16:47	17	36.0	1.3%	851,939
16:55	25	54.0	4.2%	988,797
17:03	33	72.0	9.7%	1,302,155
17:12	42	90.0	18.2%	1,960,647
17:20	50	108.0	29.7%	2,918,317
17:28	58	126.0	44.2%	4,343,799
17:37	67	144.0	61.3%	6,565,112
17:45	75	162.0	80.2%	9,147,633
17:54	84	180.0	100.0%	12,771,887
18:02	92	162.0	80.2%	12,397,322
18:10	100	144.0	61.3%	8,601,185
18:19	109	126.0	44.2%	854,789
18:27	117	108.0	29.7%	(8,663,455)
18:35	125	90.0	18.2%	(20,277,034)
18:44	134	72.0	9.7%	(33,421,077)
18:52	142	54.0	4.2%	(47,558,362)
19:00	150	36.0	1.3%	(62,231,897)
19:09	159	18.0	0.2%	(77,109,662)
19:17	167	0.0	0.0%	(92,017,100)

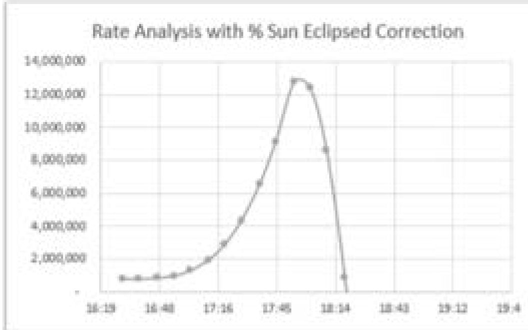

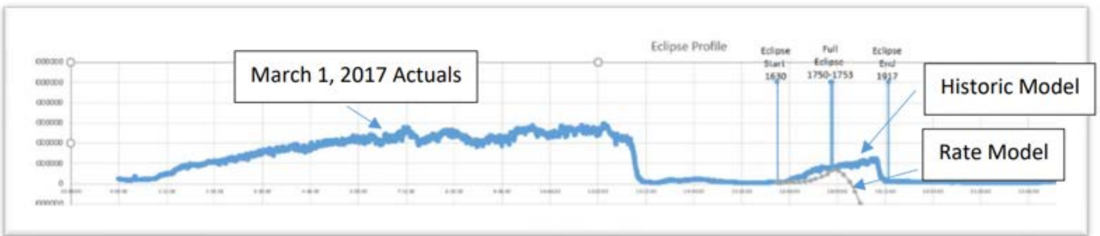

Combined Model Detail

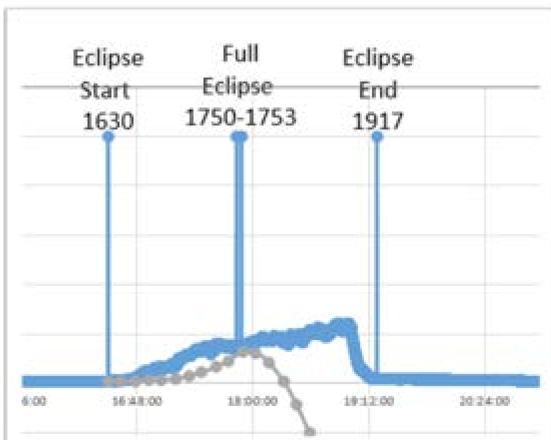

Prediction Summary

- The beginning of the eclipse has a slow increase in signal rate until full eclipse – both models correspond to the rise
- The historic data model assumes the end of the eclipse equates to the normal SuperSID levels and therefore the model – longer upward transient before sharp drop
- The rate model shows that the signal level would drop almost immediately after full eclipse.
- The SuperSID community will take data during the eclipse and the accuracy of this prediction will be validated.

August 21, 2017 SuperSID Eclipse Measurement

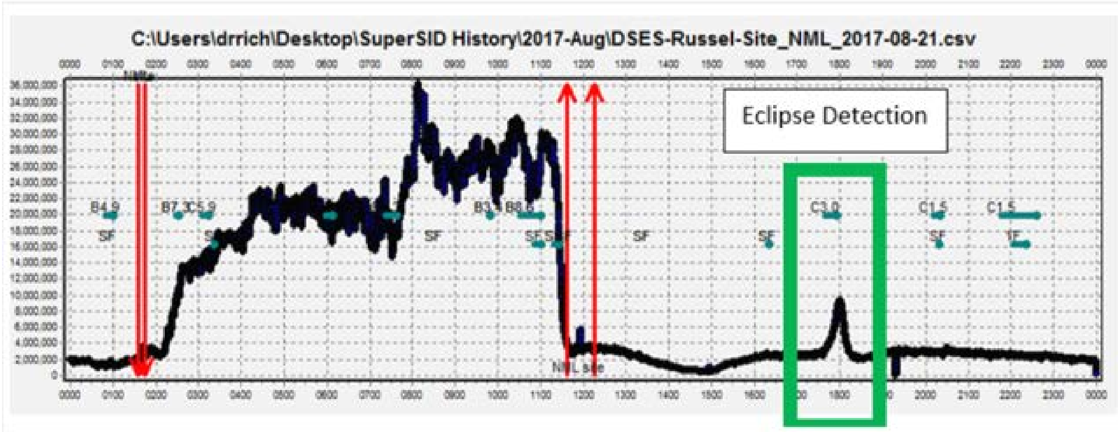

Predicted Curves vs. Actuals

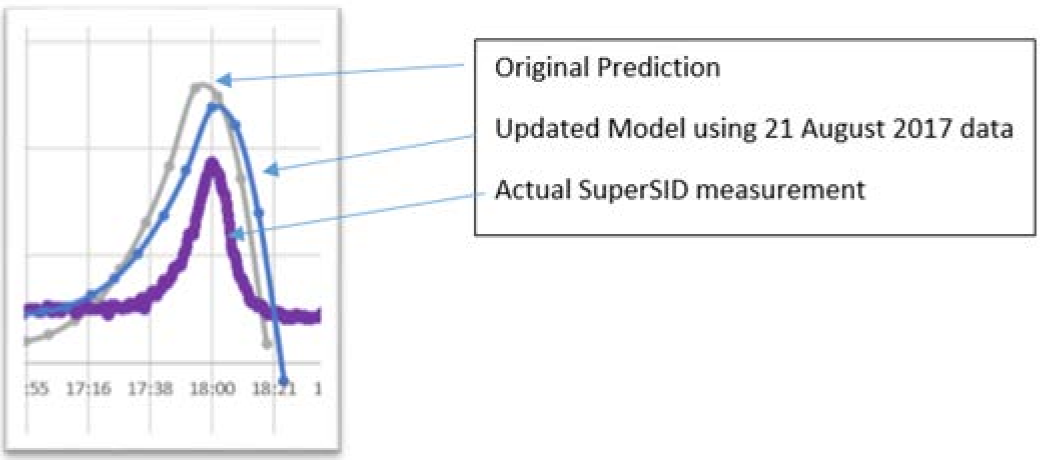

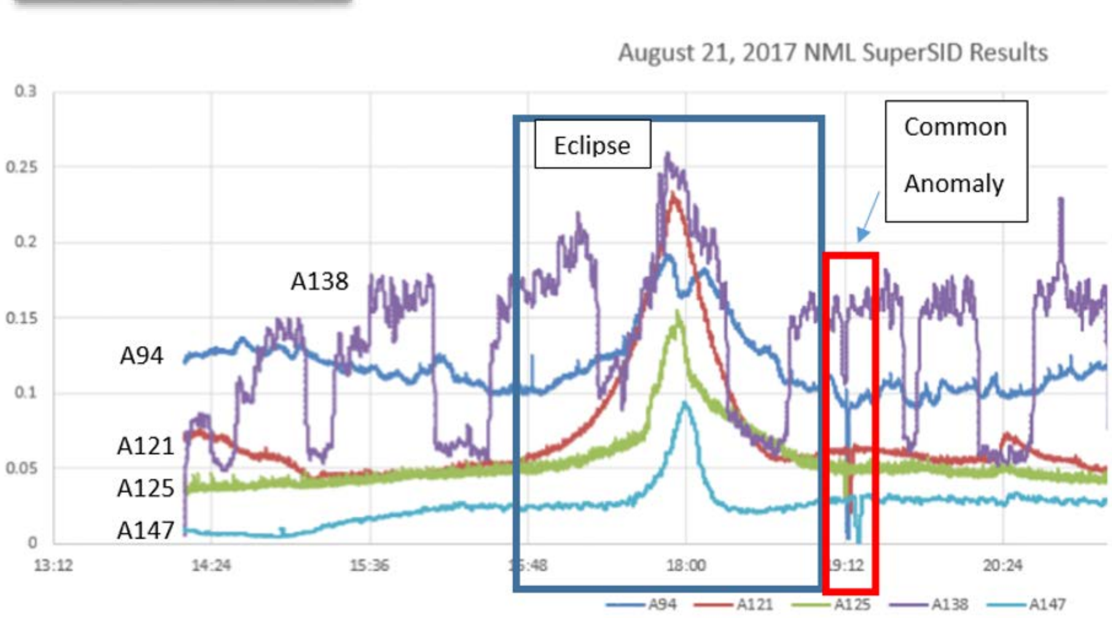

Summary

- An eclipse can be measured using the variation of ionospheric changes
- The SuperSID radio telescope is sensitive enough to observe an eclipse if the geometry of the transmitter and the eclipse path are favorable
- An eclipse signal can be predicted using basic geometry and historic sunrise and sunset historical data

AUTHOR INFORMATION

Richard A. Russel (AC0UB)

Dr. Rich Russel is the vice president for Society of Amateur Radio Astronomers (SARA) and the current science lead for the Deep Space Exploration Society (DSES). He is a retired Northrop Grumman Senior Systems Engineer and served as the Chief Architect for the Satellite Control Network Contract (SCNC). In this capacity he was charged with planning the future architecture of the Air Force Satellite Control Network (AFSCN) and extending the vision to the Integrated Satellite Control Network (ISCN). Dr. Russel has been the lead architect and integrator for the Space-Based Blue Force Tracking project for U.S Space Command, the Center for Y2K Strategic Stability, and CUBEL Peterson. Dr. Russel also has led the SPAWAR Factory team in the deployment of the UHF Follow-On Satellite system. He has a Doctorate in Computer Science, an Engineers Degree in Aeronautics and Astronautics, a Master's in Astronautical Engineering, and a Bachelor's in Electrical Engineering. He is also certified as a Navy Nuclear Engineer and he is a retired Navy nuclear fast attack submariner and Navy Space Systems Engineer.

Society of Amateur Radio Astronomers (radio-astronomy.org)

Deep Space Exploration Society (DSES.science)

ABSTRACT

The sudden ionospheric disturbance (SID) monitor measures the signal strength of a very low frequency (VLF) broadcast station after its signal is reflected off of the ionosphere. The characteristics of the signal strength is highly dependent on the local night and day. The Sun's energy ionizes the Earth's atmosphere during the day. This produces different ionization layers defined as layers D, E, F. At night, there is only ionization from cosmic waves, and therefore there is only an F layer (1). VLF radio waves reflect off the free electrons in the different ionosphere layers. The signal strength of this reflected signal can be detected by a SID small radio telescope. The normal use of the SID radio telescope is to detect solar flares which appear as short term signal strength increases during the daytime monitoring. The author used the SuperSID telescope's capability to measure and analyze the VLF signal strength variations and the effect of the solar eclipse on the ionosphere. The total solar eclipse on August 21, 2017 in North America provided an opportunity to analyze the differences between the eclipse and normal daily ionospheric reflections.

REFERENCES

1. Stanford Solar . SuperSID Manual: Space Weather Monitors. s.l. : Stanford Solar Center, Stanford University, 2009.

2. Bamford, Ruth. Radio and the 1999 UK Total Solar Eclipse. Radio Communications Agency. Chilton, UK : s.n., 2000.

3. American Association of Variable Star Observers. [Online] https://www.aavso.org/.

4. SuperSID Manual - Space Weather Monitors. Stanford University. Stanford, California : Stanford Solar Center.

5. Sky, Jim. radiosky.com. [Online] Radio Sky Publishing.

6. NASA. https://eclipse2017.nasa.gov/eclipse-who-what-where-when-and-ho. [Online]

7. https://eclipse2017.nasa.gov/sites/default/files/eclipse_full_map.pdf. [Online]

8. NASA. https://eclipse2017.nasa.gov/sites/default/files/eclipse_full_map.pd. [Online]

9. —. https://eclipse2017.nasa.gov/eclipse-who-what-where-when-and-. [Online]

10. Kohn, Ed. CliffsQuickReview: Geometry. s.l. : Wilet Publishing Inc, 2001. ISBN 0-7645-6380-7 (http://wml.scranton.edu/search/i?0764563807&startLimit=&endLimit=).

11. Pal, Sujay. Numerical Modelling of VLF Radio Wave Propagation through Earth-Ionosphere Waveguide and its application to Sudden Ionospheric Disturbances. University of Calcutta. Kolkata, India : s.n., 2013. Ph.D. Dissertation.

12. Radio emission from cosmic ray air showers Monte Carlo simulations. T. Huege, H. Falcke. July 26, 2013, Astronomy & Astrophysics.

13. Atmospheric Ozone A Meteorological Factor in Low-Frequency and 160-meter Propagation. Brown, Robert R. 2, Communications Quarterly Spring 1999, Vol. 9.